Available online at www.sciencedirect.com
ScienceDirect
Journal of Power Sources 164 (2007) 431–440
JOURNAL OF POWER SOURCES
www.elsevier.com/locate/jpowsour

Thermal and electrochemical stability of tungsten carbide catalyst supports

H. Chhina [a,b,*], S. Campbell [a], O. Kesler [c]

[a] Ballard Power Systems, 9000 Glenlyon Parkway, Burnaby, BC, Canada V5J 5J8
[b] Department of Materials Engineering, University of British Columbia, Vancouver, BC, Canada V6T 1Z4
[c] Department of Mechanical Engineering, University of British Columbia, Vancouver, BC, Canada V6T 1Z4

Received 10 October 2006; received in revised form 31 October 2006; accepted 1 November 2006

Abstract

The thermal and electrochemical stability of tungsten carbide (WC), with and without a catalyst dispersed on it, have been investigated to evaluate the potential suitability of the material as an oxidation-resistant catalyst support. Standard techniques currently used to disperse Pt on carbon could not be used to disperse Pt on WC, so an alternative method was developed and used to disperse Pt on both commercially available WC and on carbon for comparison of stability. Electrochemical testing was performed by applying oxidation cycles between +0.6 V and +1.8 V to the support-catalyst material combinations and monitoring the activity of the supported catalyst over 100 oxidation cycles. Comparisons of activity change with cumulative oxidation cycles were made between C and WC supports with comparable loadings of catalyst by weight, solid volume, and powder volume. WC was found to be more thermally and electrochemically stable than currently used carbon support material Vulcan XC-72R. However, further optimization of the particle sizes and dispersion of Pt/WC catalyst/support materials and of comparison standards between new candidate materials and existing carbon-based supports are required.

Keywords: Catalyst support; Oxidation; Tungsten carbide; Carbon; Proton exchange membrane fuel cells

1. Introduction

Proton exchange membrane fuel cells (PEMFCs) can be used for power generation in portable, stationary, and transportation applications. PEMFCs in automotive applications are expected to experience up to 30,000 start-up/shutdown cycles in their operating lifetime [1]. After shutdown, the hydrogen is removed from the stack. When hydrogen is re-introduced during start-up, electrode potentials in excess of 1.5 V may be experienced for short periods of time. This high potential leads over time to a significant degradation in the fuel cell performance due to oxidation of the carbon catalyst support. The catalyst support must be able to survive the accumulated time at these high potentials, up to 100 h, in order to provide the necessary durability. According to Mathias et al. [1], the carbon supports currently used in automotive applications (Vulcan XC-72R and Ketjen) do not meet automotive requirements for durability. It is critical, therefore, to have a catalyst support that is more stable than carbon in PEMFCs. Carbides have been used previously as catalysts [2–5] in fuel cells, but their use as catalyst supports is rarely observed. Titanium carbide (TiC) has been used as a catalyst support in PAFCs, with a high stability reported [6].

Tungsten carbide (WC) is a commercially available material often used for cutting tools. WC has the lowest electrical resistivity (conductivity = 10^5 S cm^{-1} at 20 °C) of any interstitial carbides, and therefore qualifies as the most metallic carbide. WC can be made by direct carburisation of the W metal with carbon or graphite at 1400–2000 °C in hydrogen or vacuum. The carbide formation process can also use tungsten oxide, tungstic acid, or ammonium tungstates as the starting materials [7]. This work studies the electrochemical and thermal stability of WC to evaluate its potential use as a non-carbon catalyst support for PEMFCs.

Meng and Shen [8] observed the synergistic effect of the addition of tungsten carbide supported on C (W_2C/C) to Pt catalysts

* Corresponding author at: Ballard Power Systems, 9000 Glenlyon Parkway, Burnaby, BC, Canada V5J 5J9. Tel.: +1 604 453 3834; fax: +1 604 453 3782.
E-mail address: harmeet.chhina@ballard.com (H. Chhina).

0378-7753/$ – see front matter © 2006 Elsevier B.V. All rights reserved.
doi:10.1016/j.jpowsour.2006.11.003

on the oxygen reduction reaction (ORR) in alkaline media. Lee et al. [9] studied the stability and electrocatalytic activity of WC with the addition of Ta as a catalyst. They report that studies have shown the instability of WC under acidic and oxidative conditions. The oxidation of WC by anodic polarization may proceed as [9]:

$$WC + 5H_2O = WO_3 + CO_2 + 10H^+ + 10e^- \quad (1)$$

WC + Ta and pure WC were deposited Lee et al. [9] on glassy carbon using RF sputtering. The stability and the electrochemical activity for the ORR were investigated in a solid-state cell with Nafion 117 as the electrolyte. Cyclic voltammograms (CVs) of pure WC at 30 °C and 60 °C showed an anodic peak above 0.5 V at 30 °C, and at 60 °C, larger anodic and cathodic currents were observed. The CV data showed that the Ta addition to WC resulted in no anodic peak up to 1 V at both 30 °C and 60 °C. Lee et al. [9] carried out slow scan voltammetry in both N_2 and O_2 atmospheres. Under N_2, they observed an increase in the cathodic current for pure WC, which might have occurred due to partial reduction of W(VI) oxide to W(V) oxide. The increase in cathodic current was not observed for WC + Ta catalyst under the N_2 atmosphere. The onset potential for the ORR was observed at 0.8 V versus the standard hydrogen electrode (SHE), which is 0.35 V higher than that for pure WC catalyst. From these data, they conclude that Ta addition to WC enhances its stability and electrocatalytic activity. They claim that the enhanced stability of WC with Ta catalyst compared to that of WC alone might be due to the formation of a W–Ta alloy in the WC + Ta catalyst.

Use of tungsten carbide as a fuel cell catalyst has been made in the past, but studies of its oxidation resistance as a catalyst support candidate for PEMFCs have not been reported. In order to determine the potential for WC to exhibit longer term stability in performance compared to currently used carbon supports, the thermal and electrochemical stability of WC have been evaluated ex situ in this study. Electrochemical tests involving oxidation cycling under accelerated test conditions and simulated fuel cell start-up conditions have been conducted in order to observe the oxidation stability of tungsten carbide.

2. Experimental procedure

The suitability of tungsten carbide for potential use as a catalyst support has been investigated by evaluating the electrochemical and thermal stability of tungsten carbide in ex situ tests. Commercially available tungsten carbide (Alfa Aesar) has been used. First, a new method for dispersing Pt on the candidate catalyst support material was developed, and then used to disperse Pt catalyst onto both WC and C (Vulcan XC-72R) catalyst supports for comparison. The Pt was dispersed on the C support in an amount of 40 wt%, and comparisons were made between the carbon and tungsten carbide supports after depositing Pt on tungsten carbide in three different amounts, to provide a series of comparisons with Pt/C. The Pt was deposited on WC in amounts of 40 wt%, and in equal volume percentages as that on the C support, both on a powder volume and on a solid volume basis. The thermal and electrochemical stabilities of the C and WC catalyst supports were then evaluated and compared using thermogravimetric analysis (TGA) and rotating disc electrode (RDE) studies, respectively. X-ray diffraction (XRD) and transmission and scanning electron microscopy (TEM and SEM) were used to characterize the two catalyst support materials, with and without the dispersed platinum catalyst.

2.1. Pt addition

The standard technique used at Ballard to disperse Pt on carbon could not be used to disperse Pt on tungsten carbide. Therefore, an alternative method had to first be developed. A Pt(II) salt, Pt(II) pentan-2,4-dionate (Alfa Aesar, ~48 wt% Pt), dissolved in acetonitrile, was used as the Pt precursor. It was dispersed on WC, and then later reduced under a 20 vol% H_2/balance Ar atmosphere. Pt was dispersed on both WC and on XC-72R C supports for a series of comparisons.

2.1.1. Addition of 40 wt% Pt to tungsten carbide

The thermal stabilities of Pt on C and on WC were initially compared by dispersing 40 wt% Pt on each support. Because WC has a much larger density than C, this high Pt loading represents a worst-case scenario with respect to stability of the WC support, as increased catalyst loadings have previously been found to accelerate the oxidation of the support material. To obtain 40 wt% Pt on WC, 0.50 g of Pt(II) pentan-2,4-dionate was dissolved in 110 mL acetonitrile. To this solution was added 0.36 g of Alfa Aesar WC. The solvent was allowed to evaporate, and the resulting solid was heat treated in a tube furnace at 600 °C for 5 h under 20 vol% H_2/balance Ar.

2.1.2. Pt addition to equal powder volumes of support

Similar amounts of Pt were dispersed onto supports that have a significant density difference, i.e., carbon and WC. Typically, 40 wt% Pt is dispersed on carbon catalyst supports. However, because the density difference between C and WC is large, with the materials having densities of 1.8 g cm^{-3} and 15.6 g cm^{-3}, respectively, a comparison between 40 wt% Pt on WC and 40 wt% Pt on C results in a tendency towards the observation of a lower stability of the WC, as the volumetric loading of the catalyst on WC will be higher than that on C for the same gravimetric loading. Therefore, an additional comparison was also made with a smaller volumetric loading of the catalyst on the WC support. In this comparison, 40 wt% Pt was dispersed on C, and a similar volume fraction of Pt was dispersed on the WC support material, using tapped powder densities for comparison.

Tap density is the density of a powder when the volume receptacle is tapped or vibrated under specified conditions while being loaded. Tap density was used to measure similar powder volumes of the support materials. The dispersion was performed by packing 2 mL of a support powder in a glass cylinder. The cylinder was then tapped on a counter top 200 times until 2 mL of well packed support material was obtained, as described in ASTM standards B527, D1464 and D4781. Both carbon and tungsten carbide were tapped to a volume of 2 mL. A solution of Pt(II) pentan-2,4-dionate (Alfa Aesar, ~48 wt% Pt) dissolved in 100 mL acetonitrile was prepared. To carbon, 40 wt% Pt was

added, and a similar amount of Pt as that for carbon was added to WC. The Pt(II) solution was added to the 2 mL packed support material, and the solution was then heated to 70 °C until a dry powder was achieved. The resulting solid was heat treated in a tube furnace at 600 °C for 5 h under 20 vol% H_2/balance Ar. The heat treatment resulted in Pt(II) reduction to Pt metal.

2.1.3. Pt addition to carbon and tungsten carbide in equal solid volume ratios

To take into account the different packing densities of the WC and C powders, a third comparison of the two supports was made by loading them with the same volume fraction of catalyst as is present in the standard 40 wt% carbon baseline composition, based on solid volumes of the two supports. The mass of carbon tapped to a volume of 2 mL, as described in Section 2.1.2, was 0.1140 g. Using the solid densities of carbon and WC, the amount of WC having the same solid volume was calculated to be 0.99 g. To 0.99 g of WC, the same amount of Pt was added as in Section 2.1.2 (40 wt% Pt relative to carbon). Both the Pt addition and reduction were carried out as described in Section 2.1.2.

2.2. Characterization techniques

Thermogravimetric analysis was used to determine the thermal stability of the conventional carbon support and of the tungsten carbide support material to oxidation in air flowing at 40 mL min^{-1}. The temperature was ramped from room temperature to 50 °C at 2 °C min^{-1}. The sample was held at 50 °C for 5 min to allow time for water removal. The sample was then ramped from 50 °C to 1000 °C at 2 °C min^{-1}. The data were analyzed by plotting normalized weight loss for each material versus temperature to determine the thermal stability of the supports under investigation.

X-ray diffraction was used to determine the presence of crystalline Pt on the tungsten oxide and C supports, and the average crystallite sizes. Crystallite sizes of the Pt and of the tungsten carbide were calculated using the Scherrer equation [10]:

$$t = 0.9\frac{\lambda}{\beta \cos\theta_b},$$

where t is the crystallite size in Å, λ is the wavelength (1.5406 Å in this case for Cu Kα radiation), b is the full-width at half maximum (FWHM) of a peak in the XRD spectrum, and θ_b is the diffraction angle for that peak.

To test the electrochemical stability of the catalyst supports, 20 mg of supported catalyst was dispersed in 2 mL of glacial ethanoic acid using ultrasound. Using a micropipette, 5 μL of the suspension was dispensed onto the flat surface of a polished glassy carbon (GC) rotating disc electrode. The solvent was removed gently with a hot air blower, leaving supported catalyst on the disc. Using the same micropipette, 5 μL of 5% alcoholic Nafion™ (DuPont) solution with EW of 1100 was dispensed onto the disc. The solvent was allowed to slowly evaporate in still air in a glass enclosure so that a coherent Nafion™ film was cast over the catalyst and the disc. The RDE was then immersed in deoxygenated 0.5 M H_2SO_4 at 30 °C and rotated at 33.33 Hz (2000 rpm). The electrochemical cell comprised a glass working compartment with a water jacket connected to a circulating water bath and two side compartments: one containing a Pt gauze counter electrode connected by a glass frit, and the other containing the reversible hydrogen electrode (RHE) connected by a Luggin capillary.

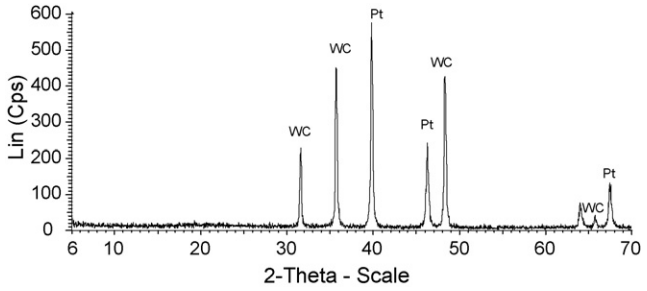

Fig. 1. XRD pattern for Alfa Aesar WC with 40 wt% Pt deposited by Pt(II) reduction to Pt, showing only reduced Pt and WC phases. Average WC crystallite size is 36 nm, and average Pt crystallite size is 30 nm.

Based on preliminary voltage cycling experimental results, the oxidation potential chosen for the electrochemical cycling tests was +1.8 V versus RHE. Above +1.8 V, considerable gas was evolved, which separated the catalyst/Nafion™ deposit from the disc. At lower potentials, the oxidation was not detectable in a suitable experimental timeframe. Using an EG&G 263 (PAR, Princeton, NJ) potentiostat with Corrware software (Scribner Associates), potential steps (oxidation cycles) between 0.6 V and +1.8 V were applied. The electrode was held at 0.6 V for 60 s and at 1.8 V for 20 s. A cyclic voltammogram (CV) was recorded between 0.0 V and 1.4 V at 100 mVs^{-1} before the oxidation cycles began and then again after every 10 oxidation cycles, until a total of 100 oxidation cycles had been applied.

A 200 kV Hitachi H-800 TEM with a Quartz XOne EDX system and a S-4700 FESEM (Field Emission Scanning Electron Microscope) were used to characterize the supported and unsupported materials. Elemental maps from EDX were used to characterize the dispersion of Pt on the supports.

3. Results and discussion

3.1. 40 wt% Pt on tungsten carbide

The XRD spectrum of Pt(II) reduced to 40 wt% Pt onto Alfa Aesar WC is shown in Fig. 1. The average crystallite size of WC calculated from the peaks at 2θ of 31.5°, 35.6° and 48.3° is 36 nm. The average crystallite size for Pt calculated from peaks at 2θ 39.8° and 46.1° is 30 nm. The average crystallite size of Pt supported on Vulcan XC-72R (Fig. 2), calculated from peaks at 2θ of 40° and 46°, is 33.6 nm. Pt deposition on both WC and Vulcan XC-72R resulted in dispersed Pt particles of similar crystallite sizes on both support materials. Although the Pt crystallite size in PEMFC catalyst layers is typically in the range of 3–10 nm, the technique commonly used to deposit Pt on C cannot be used to deposit Pt onto WC, so the new deposition technique that had to be developed was used for both WC and C

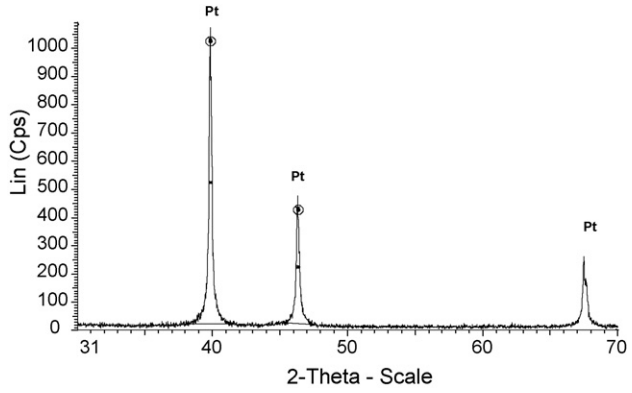

Fig. 2. XRD pattern for 40 wt% Pt on Vulcan XC-72R with Pt deposited by Pt(II) reduction to Pt. Pt crystallite size is 33.6 nm.

to allow more direct comparisons between the two supports to be made.

This work represents the first use of the new dispersion technique to deposit Pt onto WC, so the procedure cannot be considered fully optimized, in contrast with existing procedures for the dispersion of 3 nm Pt particles onto C supports, which have been in development for many years. Furthermore, a commercially available WC powder was used for this preliminary characterization study, in order to determine the electrochemical and thermal stability of the support material. It is therefore expected that further improvements in catalyst and support particle sizes will be possible once a candidate support material with adequate electrochemical and thermal stability is found, in order to improve the electrochemical activity of the new catalyst/support combination.

TGA experiments were performed to observe the materials' stability to chemical oxidation. The thermal stability data for Alfa Aesar WC, 40 wt% Pt on Alfa Aesar WC, and 40 wt% Pt on Vulcan XC-72R C are shown in Fig. 3. Pt supported on Vulcan XC-72R loses ~55 wt% of the material, which corresponds to the loss of carbon. Both Alfa Aesar WC and Pt supported on WC gained weight above ~450 °C. The gain in weight may be attributed to tungsten oxide formation. Tungsten oxide is a yellow powder, and it was observed that both Alfa Aesar WC and Pt supported on WC had turned from dark gray powders to yellow powders after the TGA run was complete. Since PEMFCs

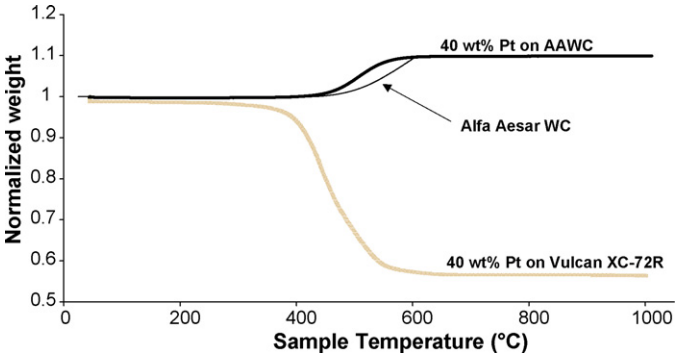

Fig. 3. TGA data for Alfa Aesar WC, 40 wt% Pt on Alfa Aesar WC and 40 wt% Pt on Vulcan XC-72R under air at 40 ml min^{-1}, with temperature ramped from 50 to 1000 °C at 2 °C min^{-1}.

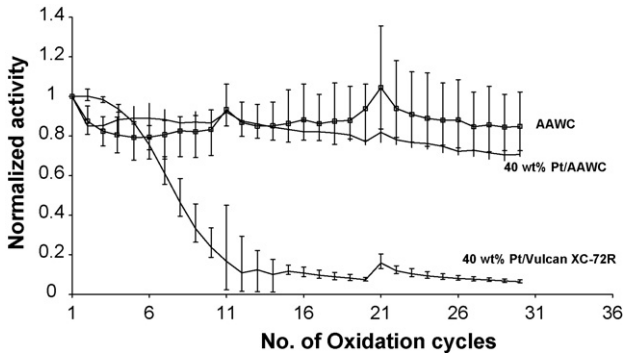

Fig. 4. Change in anodic activity at 1.8 V as a result of repeated cycling for Alfa Aesar WC, 40 wt% Pt on Vulcan XC-72R and 40 wt% Pt on Alfa Aesar WC. Average of three samples with limits of error for each material are plotted.

are low temperature operating fuel cells, the tungsten carbide oxidation will not be thermally favored. However, with the low pH and high potential conditions in PEMFCs, tungsten carbide may undergo oxidation during PEMFC operation on start-up cycles. Detailed electrochemical tests are therefore also needed to understand whether tungsten carbide oxidation is an issue for PEMFC operation.

The electrochemical stability of Alfa Aesar WC, 40 wt% Pt on Alfa Aesar WC, and 40 wt% Pt on Vulcan XC-72R were investigated by accelerated electrochemical oxidation cycling. The normalized activity as a function of number of cumulative oxidation cycles is shown in Fig. 4 for each of the three materials. The electrochemical stability as determined by accelerated testing on a RDE shows that Pt on WC and WC alone are both more stable, i.e., their electrochemical activity shows less change with oxidation cycling, than Pt supported on Vulcan XC-72R, when cycled between +0.6 V and +1.8 V.

The CV of pure Alfa Aesar WC is shown in Fig. 5. The CV after 100 cycles develops reversible peaks at 0.65 V in the anodic region and at 0.55 V in the cathodic region. The ~100 mV difference between the peaks indicates the presence of reversible solution species rather than adsorption of any species [11]. The reversible peaks may result from the formation of quinone/hydroquinone or other carbon–oxygen species, as reported elsewhere [12].

The initial CV for 40 wt% Pt supported on WC (Fig. 6) shows a sharp anodic peak above 1.2 V. The sharp anodic peak was not observed in subsequent CV scans. The oxidation of WC (Eq.

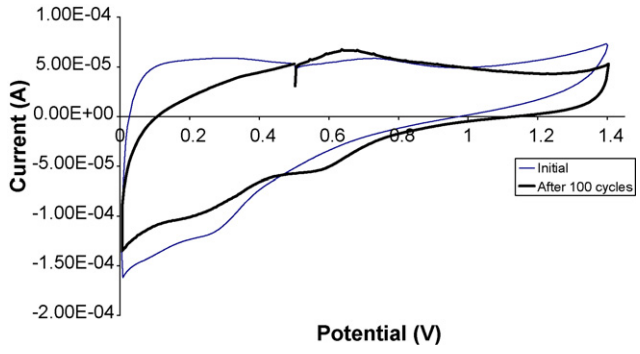

Fig. 5. Cyclic voltammograms for Alfa Aesar WC both before and after 100 oxidation cycles; 0.5 M H_2SO_4, 30 °C, 100 mV s^{-1}, 2000 rpm.

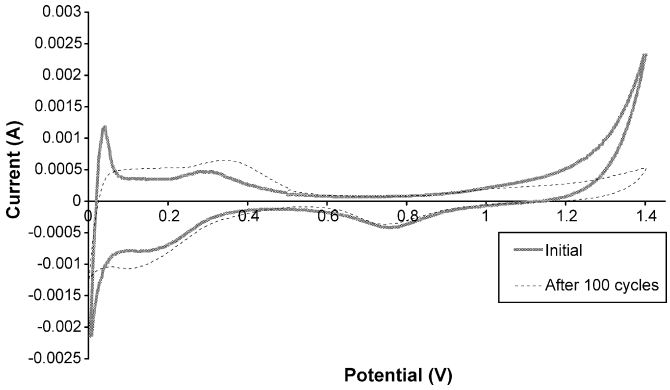

Fig. 6. Cyclic voltammograms for 40 wt% Pt on WC both before and after 100 oxidation cycles; 0.5 M H_2SO_4, 30 °C, 100 mV s^{-1}, 2000 rpm.

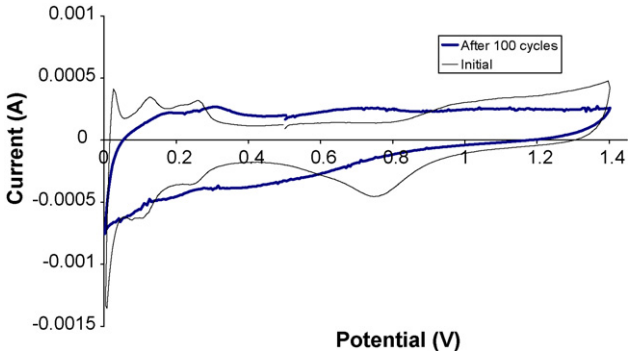

Fig. 7. Cyclic voltammograms for 40 wt% Pt on Vulcan XC-72R, both before and after 100 oxidation cycles; 0.5 M H_2SO_4, 30 °C, 100 mV s^{-1}, 2000 rpm.

(1)) by anodic polarization has been reported by Lee et al. [9]. They report that a sharp anodic peak above 0.8 V during CV of pure WC has also been observed.

In the current study, the sharp anodic peak was no longer observed after the initial CV scan. This behavior is consistent with the surface oxidation of W during the first scan, with no further oxidation during the subsequent CV scans. In that case, the structure of the support would change from Pt supported on WC to Pt supported on a WO_x shell encapsulating a WC core. Sub-stoichiometric tungsten oxide, WO_x, is a narrow-bandgap semiconductor with reasonable electronic conductivity.

In addition, on the positive scan, a broad peak between 0.3 V and 0.45 V with no apparent counter-part on the negative scan is observed. Similar results have been reported by other researchers [13,14]. Tungsten oxide forms two stable hydrogen tungsten bronzes, $H_{0.18}WO_3$ and $H_{0.35}WO_3$, and sub-stoichiometric oxides, WO_{3-y}, by reaction with hydrogen [13]:

$$WO_3 + xH^+ + xe^- = H_xWO_3 \quad (0 < x < 1) \tag{2}$$

$$WO_3 + 2yH^+ + 2ye^- = WO_{3-y} + yH_2O \quad (0 < y < 1) \tag{3}$$

Also, hydrogen spill-over from Pt has been reported [13]:

$$xPtH_{ads} + WO_3 = Pt + H_xWO_3 \tag{4}$$

$$H_xWO_3 = xH^+ + WO_3 + xe^- \tag{5}$$

The increase in the hydrogen adsorption/desorption peak area, along with the formation of a broad anodic peak between

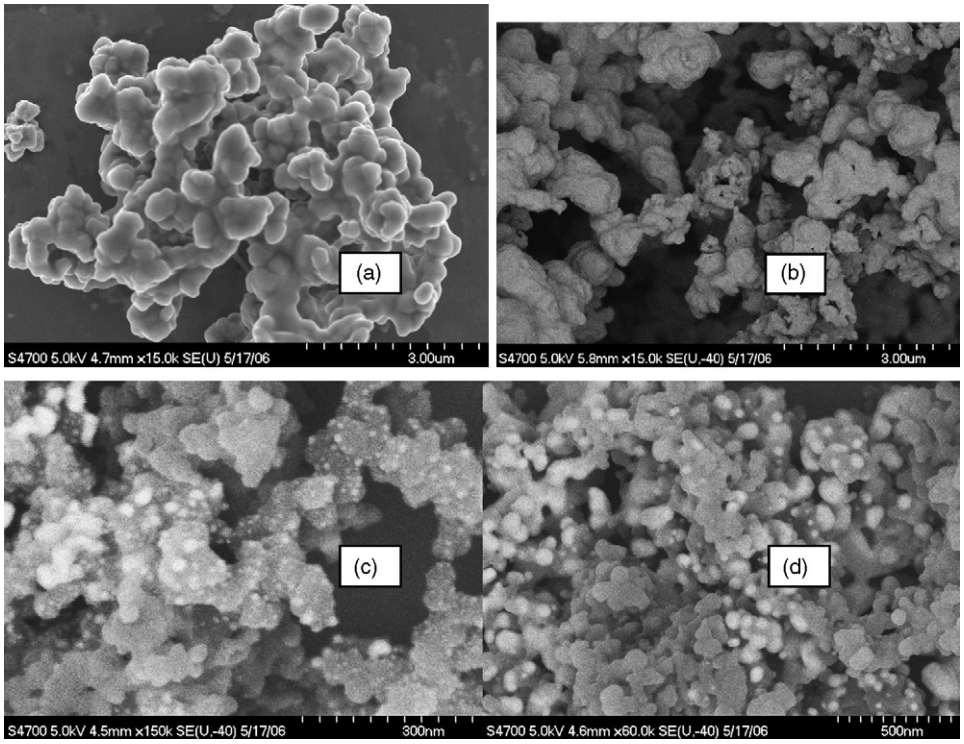

Fig. 8. SEM images of 40 wt% Pt dispersed onto catalyst supports by reduction from Pt(II) pentan-2,4 dionate. (a) Pt on WC, secondary electron mode, (b) Pt on WC, mixed secondary and backscattered electron mode, (c) Pt on C, mixed secondary and backscattered electron mode, (d) Pt on C, secondary electron mode. Pt and C exhibit a higher contrast compared to Pt and W due to the larger differences in atomic number, making SEM less suitable for determination of particle sizes in the Pt/WC system compared to the Pt/C system.

0.3 V and 0.45 V, probably occurs due to tungsten bronze formation [13], and therefore can not be used on its own as a measure of electrochemical activity to determine electrochemically active surface area [14]. These results suggest that WC is likely oxidizing under the current electrochemical conditions used to test the stability of this support material. Therefore, tungsten carbide might not be stable under PEMFC conditions and may oxidize to WO_x with operation. However, the platinum oxide reduction peak at ~0.75 V does not decrease in area even after 100 oxidation cycles for Pt/WC (Fig. 6), indicating that the catalyst/support combination may retain sufficient activity even if the WC is oxidizing to semiconducting WO_x on its surface. Because the hydrogen adsorption/desorption peak is likely to correspond to the formation of hydrogen bronze in this system, the presence of a distinguishable platinum oxide reduction peak has been used instead to indicate whether a significant amount of platinum is present on the surface that can participate in the catalysis of the oxygen reduction reaction. Since Pt remains active on the surface of the electrochemically cycled Pt/WC material, the extent of oxidation during operation and the impact on fuel cell performance need to be studied further before ruling out the option of using WC as a catalyst support in PEMFCs. In contrast, the Pt reduction peak is completely lost after 100 oxidation cycles for Pt supported on Vulcan XC-72R (Fig. 7).

An SEM image of 40 wt% Pt on Alfa Aesar WC shows the presence of dense spheres packed together with some irregularly shaped particles (Fig. 8a and b). It is difficult to distinguish between Pt and WC particles in the high-resolution SEM images of the Pt on WC. An SEM image of Pt on Vulcan XC-72R (Fig. 8c) shows fine Pt particles dispersed on carbon. Pt particle sizes ranging from 10 nm to 60 nm are observed for Pt/C in the SEM micrographs, while the crystallite sizes as determined by XRD averaged 34 nm. The average crystallite size for WC was calculated to be 36 nm from the XRD results, with the supported Pt on WC having an average crystallite size of 30 nm. In contrast, state of the art crystallite sizes range from 3 nm to 10 nm on commercial carbon supports. Therefore, the Pt particle size needs to be further optimized to improve performance.

A TEM image of 40 wt% Pt dispersed on Alfa Aesar WC is shown in Fig. 9. The elemental spectrum along with the concentrations for spots 1 and 2 on the TEM image show that the darker area (spot 1) has a Pt:W ratio of 0:100, and spot 2 has a Pt:W ratio of 22:78 by weight. It is difficult to distinguish between Pt and WC in TEM images, but the elemental maps can be used to obtain

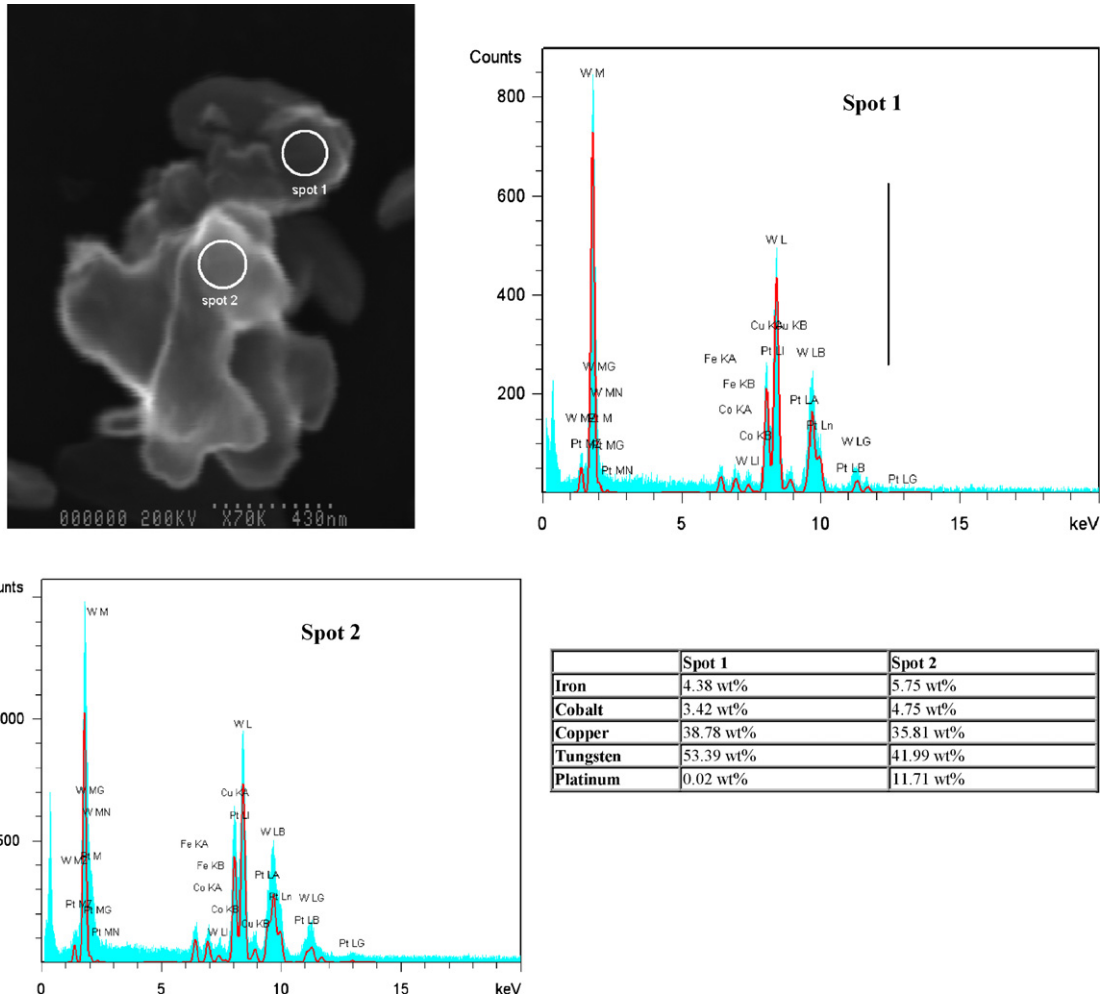

	Spot 1	Spot 2
Iron	4.38 wt%	5.75 wt%
Cobalt	3.42 wt%	4.75 wt%
Copper	38.78 wt%	35.81 wt%
Tungsten	53.39 wt%	41.99 wt%
Platinum	0.02 wt%	11.71 wt%

Fig. 9. TEM images and EDX results of 40 wt% Pt dispersed on Alfa Aesar WC using Pt(II) pentan-2,4-dionate. Elemental spectrum and weight concentration for spots 1 and 2 on the TEM image are shown.

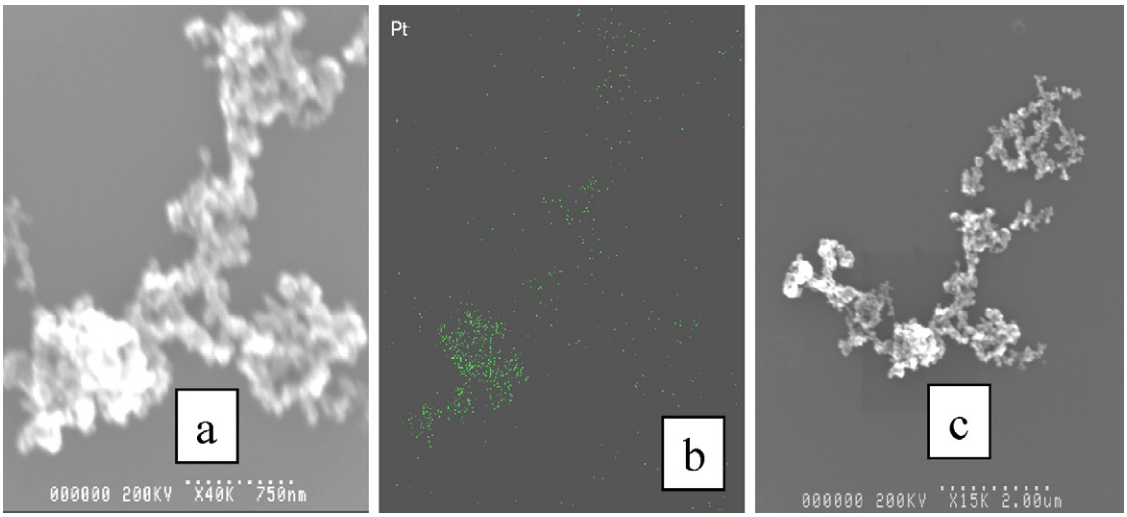

Fig. 10. TEM images and Pt elemental map of 40 wt% Pt dispersed on Vulcan XC-72R using Pt(II) pentan-2,4-dionate. (a) High-magnification image, (b) elemental Pt map and (c) low magnification image.

the relative ratios of each element. The presence of iron, cobalt, and copper results from the sample holder. These compositional breakdowns show that Pt is dispersed in discrete particles on the support material. TEM images and an elemental map of 40 wt% Pt/Vulcan XC-72R (Fig. 10), show the presence of Pt clusters dispersed on carbon. The dispersion technique needs to be optimized so that finer Pt particles can be more evenly dispersed on the support material. For example, liquid nitrogen could be used to rapidly quench chlorplatinic acid into well-dispersed solid particles over a catalyst support, which could then be reduced to Pt in situ, as reported by Hobbs and Tseung [15].

3.2. Comparison of Pt deposited using Pt(II) pentan-2,4-dionate on similar powder volumes of Alfa Aesar WC and Vulcan XC-72R

In order to examine the effects of different catalyst loadings on the WC catalyst support electrochemical stability, additional tests were performed on Pt deposited on a WC support in the same volume ratio according to total powder volume as on the C support having a gravimetric loading of 40 wt% Pt. Since carbon can be made by many methods that result in different morphologies, the tap density is usually used to characterize the density of these carbon support materials.

CV tests repeated on the 40 wt% Pt/Vulcan XC-72R standard demonstrated a complete loss of the Pt oxide reduction peak after 100 oxidation cycles, as in the previous tests. However, The CV of the Pt deposited on WC (Fig. 11) showed no significant Pt activity before or after cycling, and the XRD pattern of the as-reduced Pt/WC sample made with an equal volume fraction of Pt/powder as in the Pt/C showed that the amount of Pt present on the support material after reduction was below the standard 5% detection limit for the XRD (Fig. 12), with only a very small peak visible slightly above the baseline at the angle $2\theta = 39.8^\circ$ corresponding to the highest intensity Pt peak.

The CV for Pt/WC (Fig. 11) does not exhibit any Pt characteristics, such as hydrogen adsorption/desorption or Pt oxidation/Pt

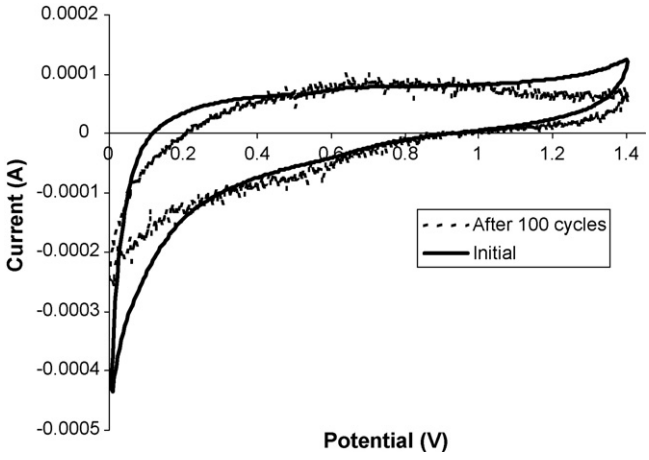

Fig. 11. Cyclic voltammograms for 0.91 wt% Pt dispersed on Alfa Aesar WC, initially and after 100 oxidation cycles; 0.5 M H_2SO_4, 30 °C, 100 mV s^{-1}, 2000 rpm. Pt loading corresponds to same volume fraction of Pt/total powder volume for both Pt/WC and for 40 wt% Pt/C.

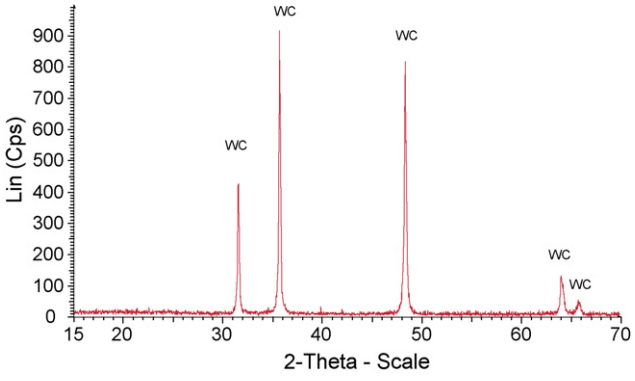

Fig. 12. XRD pattern for Alfa Aesar WC with 0.91 wt% Pt deposited from Pt(II) by reduction to Pt. Catalyst loading corresponds to same catalyst/powder volume ratio as in 40 wt% Pt/C.

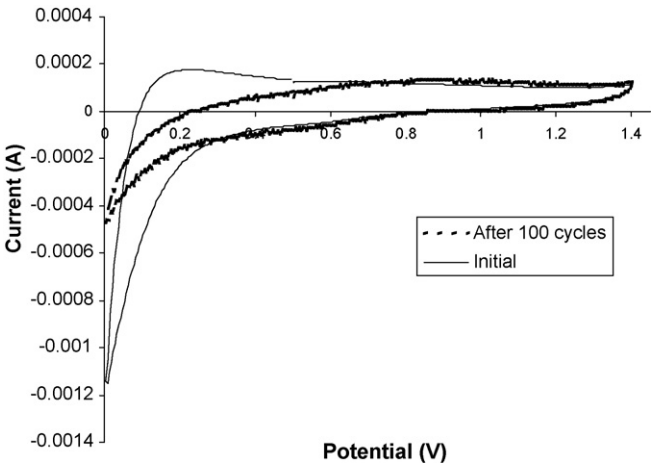

Fig. 13. Cyclic voltammograms for 6 wt% Pt dispersed on Alfa Aesar WC, initially and after 100 oxidation cycles; 0.5 M H_2SO_4, 30 °C, 100 mV s^{-1}, 2000 rpm. Catalyst loading corresponds to equal solid volume ratio of Pt/WC as in 40 wt% Pt/C.

oxide reduction, and only a very faint Pt peak of the highest intensity was observed in the CV or in the XRD pattern. Therefore, Pt crystallite size on the WC support could not be determined from the XRD data, although any Pt present may potentially have the same average crystallite size due to the identical deposition/dispersion technique as that used to deposit 40 wt% Pt on both C and WC.

Similar packing techniques were used in packing both the Vulcan XC-72R and WC powders to a volume of 2 mL. However, WC, as a very dense material with a small crystallite size (~36 nm), packs more densely compared to the C particles, which have a less dense and more fractal-like morphology. The WC therefore has a very high surface area per unit of packed powder volume, making the quantity of Pt required to match the volumetric loading on the C powder insufficient to provide good catalytic activity. Further work is therefore required to improve the surface dispersion of the Pt on the WC, in order to provide comparable activity to that of Pt on C for a given powder volumetric loading.

3.3. Comparison of Pt deposited using Pt(II) pentan-2,4-dionate on similar solid volumes of Alfa Aesar WC and Vulcan XC-72R

To account for the differences in both solid densities and packing densities of the two support material powders, the stability of the WC and C supports was also compared with similar solid volume ratios of Pt to support material deposited on each. Using the same weight ratio of Pt to C (40 wt%) used in each of the three comparisons, the amount of WC required to obtain equal solid volume ratios of Pt to both C and WC was calculated and deposited on the WC support. The CV for Pt/WC in this case (Fig. 13) does not exhibit any Pt characteristics, such as hydrogen adsorption/desorption or Pt oxidation/Pt oxide reduction. However, there are low intensity Pt peaks observed in the XRD pattern (Fig. 14). Equal solid volume ratios result in 6 wt% Pt on WC, which is within the XRD detection limit. However, the effect of Pt was not observed in the cyclic voltammogram,

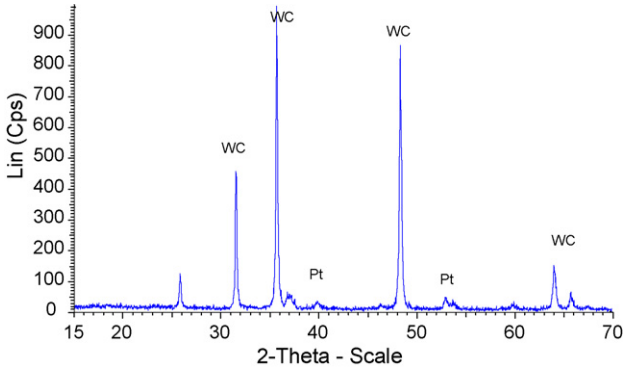

Fig. 14. XRD pattern for Alfa Aesar WC with 6 wt% Pt deposited from Pt(II) by reduction to Pt. Catalyst loading corresponds to same catalyst/solid volume ratio of Pt/WC as in 40 wt% Pt/C.

indicating that the surface area of the catalyst on the WC was likely insufficient to provide significant electrochemical activity, even when the catalyst was present in an equal volume ratio as on the C support. In the case of carbon, as before, all activity was lost after 100 oxidation cycles.

3.4. Comparison standards for new catalyst support candidate materials

When 40 wt% Pt was dispersed on WC, the Pt:WC solid volume ratio was ~0.49, which was much higher than the Pt:C solid volume ratio of ~0.05 corresponding to the same gravimetric Pt loading. Despite the high volumetric dispersion of Pt on WC, both the cyclic voltammetry and oxidation cycle data showed that the WC support material was more stable both thermally and electrochemically with accelerated oxidation cycling when compared to carbon with comparable Pt particle sizes on each material. Although increased levels of catalyst loading tend to accelerate the oxidation of carbon catalyst supports, even the higher volumetric loading of Pt on the WC compared to the C studied here did not lead to a substantial drop in activity during rotating disc electrode studies of the Pt/WC, while the Pt/C lost almost all of its activity after only 20 accelerated oxidation cycles.

However, despite the higher electrochemical stability of the 40 wt% Pt/WC (the catalyst loading expected to lead to the lowest stability on the WC of those studied here), compared to 40 wt% Pt/C, the problem remains of increasing the surface area of the Pt particles that are dispersed on the support, in order to increase the electrochemical activity of the catalyst/support combination. For example, much smaller volumetric loadings of Pt/WC, corresponding to the same volumetric loadings as 40 wt% Pt/C on a powder volume and on a solid volume basis, did not result in sufficient catalytic activity in the Pt/WC materials in order to result in significant Pt oxide reduction peak activity in the cyclic voltammograms, even though small quantities of Pt were detectable by XRD in the case of the 6 wt% Pt/WC, and only extremely small quantities of Pt were present in the case of 0.91 wt% Pt/WC.

The WC support material used in this preliminary material screening study was a commercially available powder with average agglomerate sizes ranging from 100 nm to 500 nm,

while the commercially available carbon material commonly used as a PEMFC catalyst support had smaller particle sizes, typically below 100 nm. As a result of the larger WC particle sizes, similar volumetric loadings of catalyst likely did not result in comparable catalyst loadings on an equal surface area basis, thus leading to a lower activity than one would obtain from a similar volume fraction of catalyst dispersed more evenly on a carbon support with smaller particles.

Therefore, despite the higher electrochemical stability of WC compared to C with equal gravimetric Pt loadings, the feasibility of utilizing WC as a catalyst support depends also on being able to produce the powder with smaller particle sizes and on achieving a higher degree of catalyst dispersion on the particles. As the commercially available WC powder available for this study has not been optimized for application as a catalyst support material, possible routes to decreasing the particle size could include mechanical processing of the powder, such as high-energy ball milling, or the synthesis of WC from high surface area C using wet chemical techniques with the addition of W from chemical precursors. Decreasing the particle size of the WC support material, combined with optimization of the Pt dispersion technique, would be required in order for the Pt/WC supported catalyst material to exhibit sufficient catalytic activity to be competitive with existing Pt/C systems. Nevertheless, the increased thermal and electrochemical stability of the WC relative to C may make such efforts worthwhile from the perspective of improving the long-term durability of PEMFC cathodes in practical applications, even if such increases in lifetime come at a cost of a somewhat lower initial catalytic activity.

The results presented here also demonstrate the inherent difficulties present in directly comparing the activities of two different catalyst support materials having very different physical properties, such as density. While different carbon–based supports (e.g., graphitized versus non-graphitized) are traditionally compared with each other under conditions of constant gravimetric catalyst loading (40 wt% Pt/C), the consideration of alternative materials with higher stability compared to that of carbon requires more caution when making comparisons of the activity and stability of the materials. Supported catalysts with fixed gravimetric and volumetric loadings can be produced directly for comparisons on these bases. However, a comparison of catalysts on the basis of surface area of support covered with catalyst compared to the total surface area of the support could in theory provide a more material-specific comparison of the properties, although gravimetric and volumetric comparisons may be of more interest for a specific application in terms of weight and space constraints. Unfortunately, production routes to synthesize different materials with identical surface areas of both support particles and catalyst particles for a comparison on that basis do not presently exist for porous, three dimensional electrodes.

Although standardized techniques for producing different supported catalysts with identical surface areas are not available, Brunauer–Emmett–Teller (BET) surface area measurements can be used to determine the total surface area available in both C and WC supports once they have produced to facilitate comparisons on a surface area basis. However, even this approach has drawbacks, because carbon is known to have internal microporosity that can be measured by BET (via N_2 adsorption), but which is not available for Pt deposition. Therefore, the actual surface area of Pt that can be supported on carbon will be lower than that which can be measured by BET. Mercury porosimetry can be used instead to determine the pore volume of a three dimensional catalyst support down to the microporosity level. However, high pressures are required for mercury to fill in the smallest pores, and this high pressure mercury infiltration could lead to ruptured carbon particles, thereby changing the morphology that is being measured. Furthermore, measurements of surface area or of internal pore volume by BET or mercury porosimetry, respectively, cannot directly distinguish between Pt and support surface area, thus leaving open the question of whether the catalyst dispersion techniques lead to identical catalyst surface areas on two different supports. Therefore, even comparisons based on a normalization of the Pt content per unit surface area of the support cannot be performed directly at present. However, electrochemical stability data based on similar quantities of Pt dispersed by the same technique on similar surface area supports could provide additional insight into the electrochemical performance and stability of alternative catalyst support materials.

4. Conclusions and future work

A series of experiments has been performed to investigate the potential suitability of WC for use as a PEMFC cathode catalyst support, with comparisons made to Vulcan XC-72R carbon supports. In each case, the standard catalyst loading of 40 wt% Pt was added to the C using a new Pt dispersion technique developed to allow comparison with WC, and equal weight, solid volume and tapped powder volume fractions of Pt were added to the WC using the same dispersion method. Despite the higher content of Pt by volume in the case of 40 wt% Pt on WC compared to C, the electrochemical stability of this support was still significantly higher than that of carbon in accelerated oxidation cycling tests with a rotating disc electrode. The electrochemical activity of the Pt/WC remained nearly constant over 100 accelerated oxidation cycles, while the activity of Pt/C was almost completely lost after only approximately 20 oxidation cycles. However, the initial activity of the Pt/WC supported catalyst is much lower than that of Pt/C at comparable volumetric catalyst loadings, indicating that higher surface area WC supports and better platinum dispersion techniques are still required in order to enhance the catalyst layer activity.

Despite the lower electrochemical activity of the Pt/WC compared to that of Pt/C, there is still a potential for its use as a catalyst support, given the severe long-term stability problems of Pt/C supported catalyst, despite the much higher short-term performance. If carbon from the support oxidizes, it is lost as carbon dioxide gas, causing Pt to fall off the support, and leading to low Pt surface area and rapid significant performance degradation in a PEMFCs. However, even if tungsten carbide oxidizes to sub-stoichiometric tungsten oxide on the particle surface, it remains moderately conductive, and little loss in Pt surface area results. Therefore, WC may have potential for use as a PEMFC cathode catalyst support, provided that a method of producing

both the support and dispersed catalyst with higher surface area and smaller particle sizes can be achieved. In the consideration of any new catalyst support material, the differences in density between the candidate material and standard C-based supports must be taken into account when any comparisons in activity or stability are made, in order to better understand the inherent differences in performance and durability of the materials.

Acknowledgements

The authors gratefully acknowledge research funding from the Advanced Systems Institute of British Columbia (ASI BC) and from the Natural Science and Engineering Research Council (NSERC) of Canada Industrial Postgraduate Scholarship (IPS).

References

[1] M. Mathias, R. Makharia, H. Gasteiger, J. Conley, T. Fuller, C. Gittleman, S. Kocha, D. Miller, C. Mittesteadt, T. Xie, S. Yan, P. Yu, Interface 14 (2005) 24–35.
[2] C. Ma, Y. Gan, Y. Chu, H. Huang, D. Chen, B. Zhou, Trans. Nonferr. Met. Soc. Chin. 14 (2004) 11–14.
[3] C. Ma, W. Zhang, D. Chen, B. Zhou, Trans. Nonferr. Met. Soc. Chin. 12 (2002) 1015–1019.
[4] J.B. Christian, R.G. Mendenhall. [US 6,656,870 B2], 2003.
[5] J.B. Christian, T.A. Dang, R.G. Mendenhall. [US 6,551,569 B1], 2003.
[6] V. Jalan, D.G. Frost. [4,795,684], 1989.
[7] H.O. Pierson, Handbook of Refractory Carbides and Nitrides, Noyes Publications, 1996, pp. 1–115.
[8] H. Meng, P.K. Shen, Chem. Commun. 2005 (2005) 4408–4410.
[9] K. Lee, K. Ishihara, S. Mitsushima, N. Kamiya, K. Ota, Electrochim. Acta 49 (2004) 3479–3485.
[10] B.D. Cullity, Elements of X-Ray Diffraction, Addison Wesley Publishing Company, Inc., 1978, pp. 1–30.
[11] R. Greef, R. Peat, L.M. Peter, J. Robinson, D. Pletcher, Instrumental Methods in Electrochemistry, Ellis Horwood limited, 1985.
[12] K. Kangasniemi, D. Condit, T. Jarvi, J. Electrochem. Soc. 151 (2004) E125–E132.
[13] J. Shim, C.R. Lee, H.K. Lee, J.S. Lee, E.J. Cairns, J. Power Sources 102 (2001) 172–177.
[14] P.J. Kulesza, L.R. Faulkner, J. Electrochem. Soc. 136 (1989) 707–713.
[15] B.S. Hobbs, A.C.C. Tseung, J. Electrochem. Soc. 119 (1972) 580–583.